Supplement of Atmos. Chem. Phys., 26, 4901–4915, 2026
https://doi.org/10.5194/acp-26-4901-2026-supplement

Atmospheric Chemistry and Physics
Open Access
EGU

Supplement of

Impact of primary oxygenated volatile organic compounds on ozone formation in the Yangtze River Delta region

Xun Li et al.

Correspondence to: Jingyi Li (jingyili@nuist.edu.cn)

S1. Model evaluation

The Pearson correlation coefficient (R), mean bias (MB), mean error (ME), normalized mean bias (NMB), normalized mean error (NME), root mean square error (RMSE), and index of agreement (IOA) were used to evaluate the model's performance in simulating meteorological parameters and air pollutants. These statistical metrics were calculated as follows:

$$R = \frac{\sum(Pi - \overline{P}) \times (Oi - \overline{O})}{\sqrt{\sum(Pi - \overline{P})^2 \times \sum(Oi - \overline{O})^2}} \quad \text{(S1)}$$

$$MB = \frac{1}{N}\sum(Pi - Oi) \quad \text{(S2)}$$

$$ME = \frac{1}{N}\sum|Pi - Oi| \quad \text{(S3)}$$

$$NMB = \frac{\sum(P\text{i-Oi})}{\sum Oi} \quad \text{(S4)}$$

$$NME = \frac{\sum|Pi - Oi|}{\sum Oi} \quad \text{(S5)}$$

$$RMSE = \sqrt{\frac{1}{N}\sum(Pi - Oi)^2} \quad \text{(S6)}$$

$$IOA = 1 - \frac{\sum(Pi - Oi)^2}{\sum(\left|Pi - \overline{O}\right| + \left|Oi - \overline{O}\right|)^2} \quad \text{(S7)}$$

where P and O represent the predicted and observed values, respectively; the subscript i denotes the i^{th} data point in a dataset of size N; $\overline{P}$ and $\overline{O}$ indicate the mean values of predictions and observations, respectively. NMB and NME were calculated without conversion to percentage form and are reported as fractions.

Hourly averages of temperature (T), relative humidity (RH), wind speed (WS), and wind direction (WD) from model simulations and observations at Xujiahui Station (Shanghai), Maigaoqiao Station (Nanjing), Mingzhu Square Station (Hefei), and Binjiang Station

(Hangzhou) in EP1 and EP2 are shown in Figs. S2 and S3, respectively. Among these four meteorological parameters, temperature was reproduced most accurately, with high R (> 0.8) and IOA (approaching 1.0) values as shown in Table S3. The model also performed reasonably well for RH, showing R > 0.68 and ME < 14%. For wind fields, the model generally captured both spatial and temporal variations, but tended to overestimate WS across all cities in both episodes, except in Hefei (HF). The agreement between predictions and observations was stronger in EP1 than in EP2. A similar pattern was observed for WD, which was better reproduced in EP1. Statistical metrics for T and WS met benchmark thresholds in most cities, indicating satisfactory model performance.

Comparisons between modeled and observed MDA8 ozone concentrations in representative cities of the YRD during the two episodes are shown in Figs. S4 and S5, respectively. The model generally reproduced the temporal variations at most stations, with IOA values exceeding 0.5 (Table S4). Peak concentrations were captured more accurately in EP2 than in EP1. However, the model tended to overestimate ozone levels below 40 ppb toward the end of EP1 and throughout EP2. This bias likely reflects limitations in the model's ability to represent background ozone. Additional contributions to this overestimation may arise from uncertainties in VOC and NO_x emissions in the current inventory.

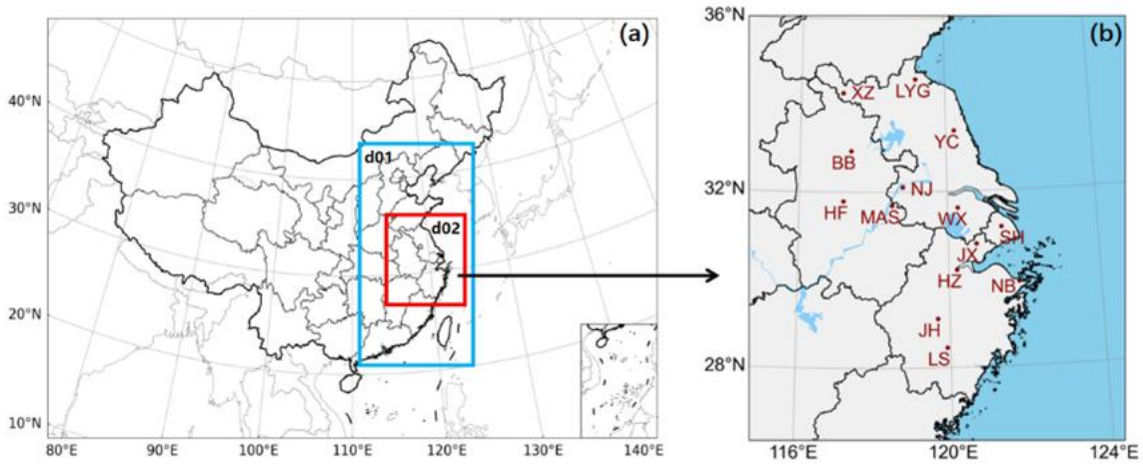

Figure S1. Simulation domains of CMAQ.

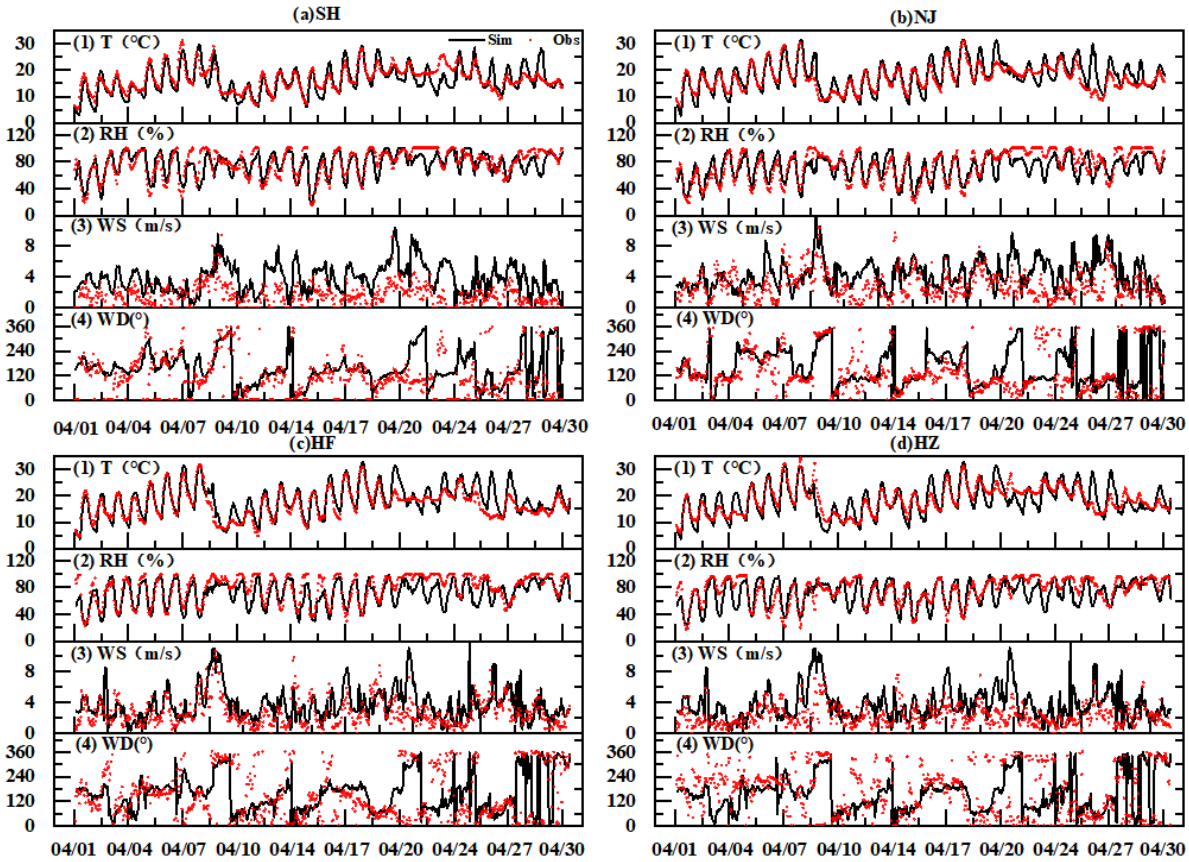

Figure S2. Comparison of simulated and observed temperature (T), relative humidity (RH), wind speed (WS), and wind direction (WD) at stations in Shanghai (SH), Nanjing (NJ), Hefei (HF), and Hangzhou (HZ) in April 2019 (EP1).

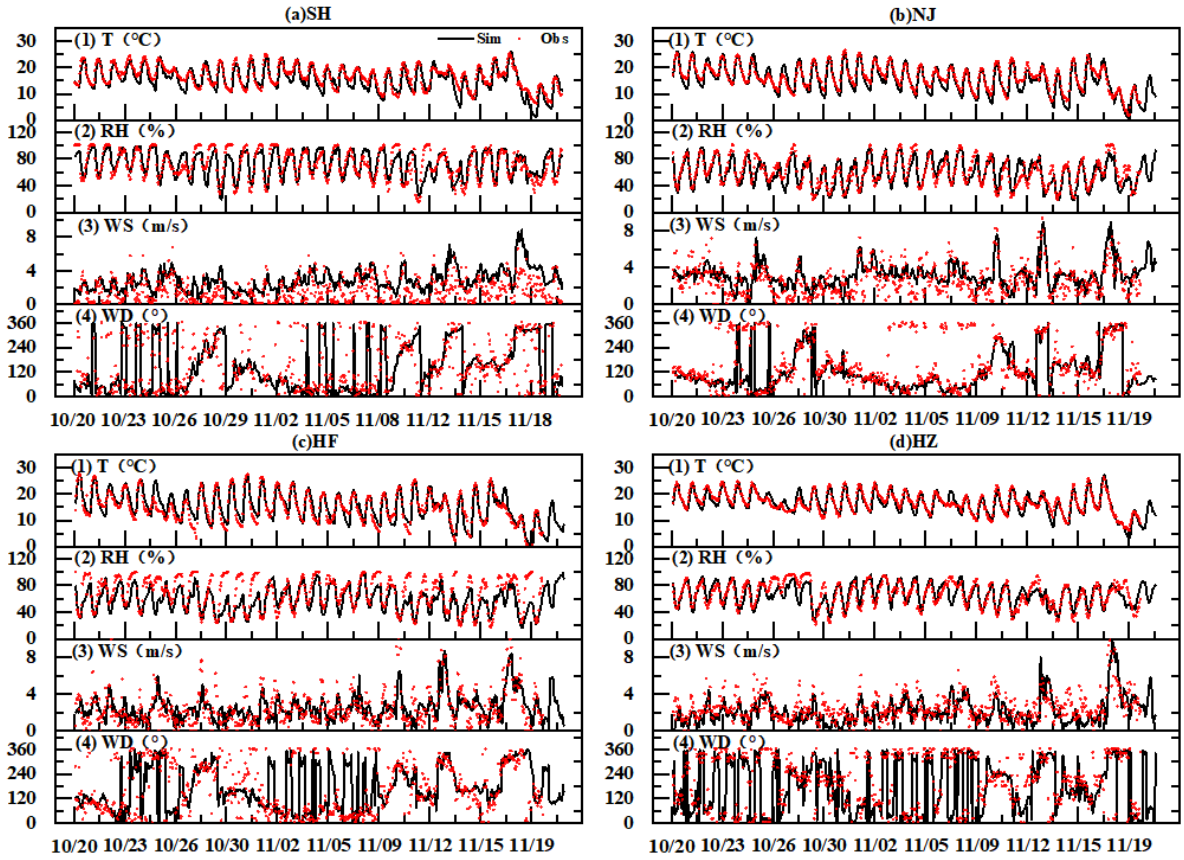

Figure S3. Same as Fig. S2, but for October−November 2019 (EP2).

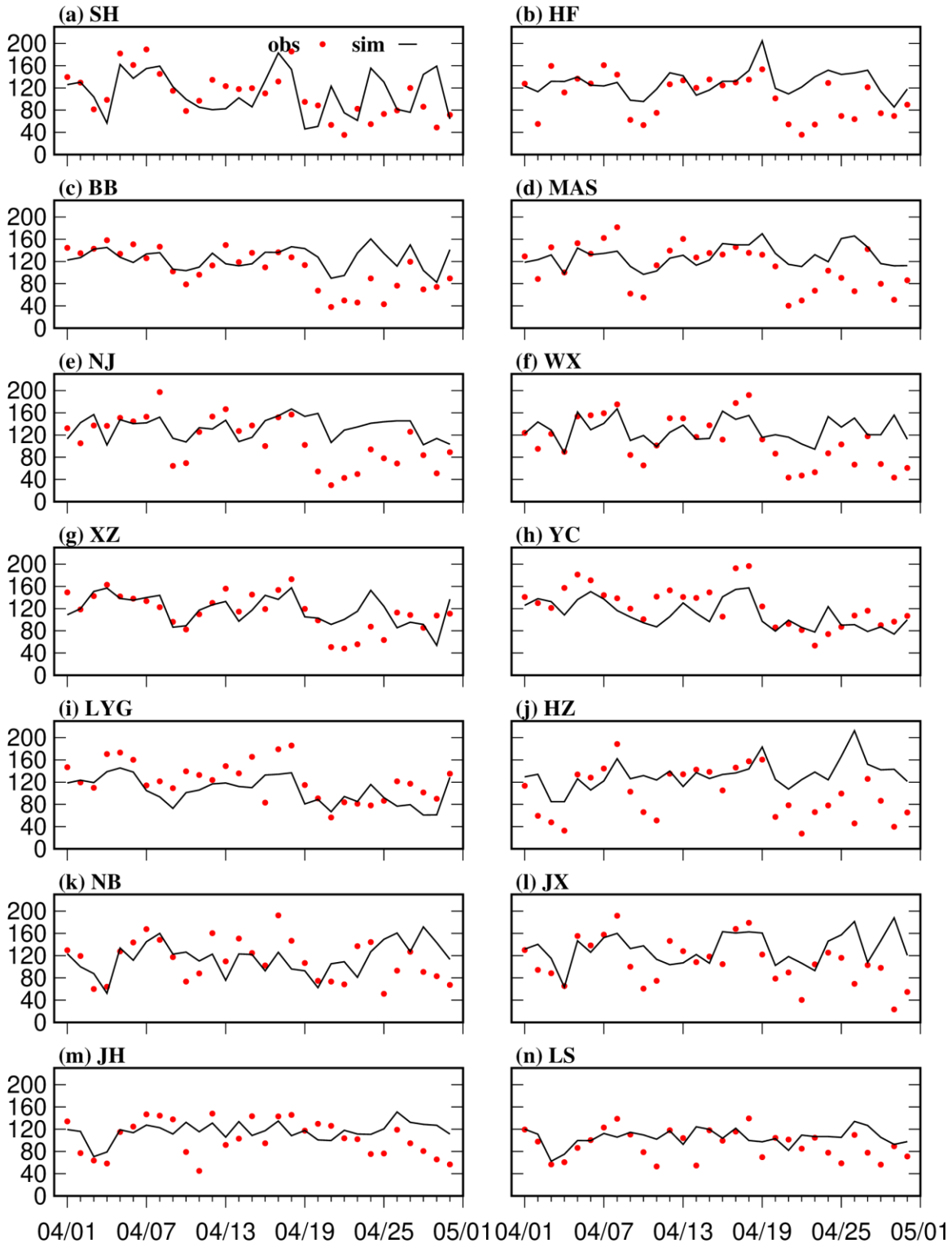

Figure S4. Temporal variations of MDA8 ozone concentrations across selected cities in the YRD region in EP1 (μg m^{-3}).

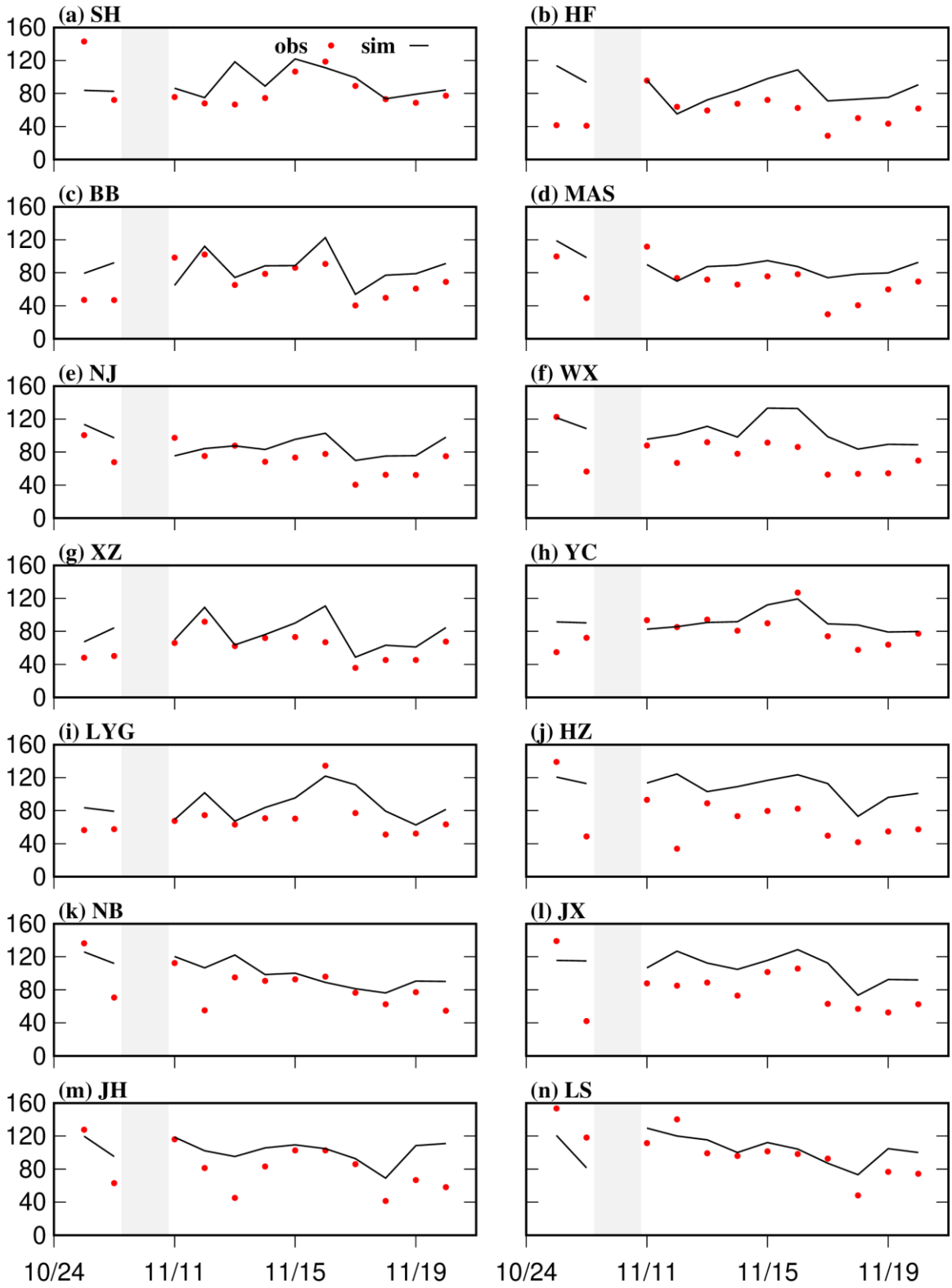

Figure S5. Same as Fig. S4, but for October−November 2019 (EP2). Gray shaded areas denote the China International Import Expo 2019 (CIIE) period.

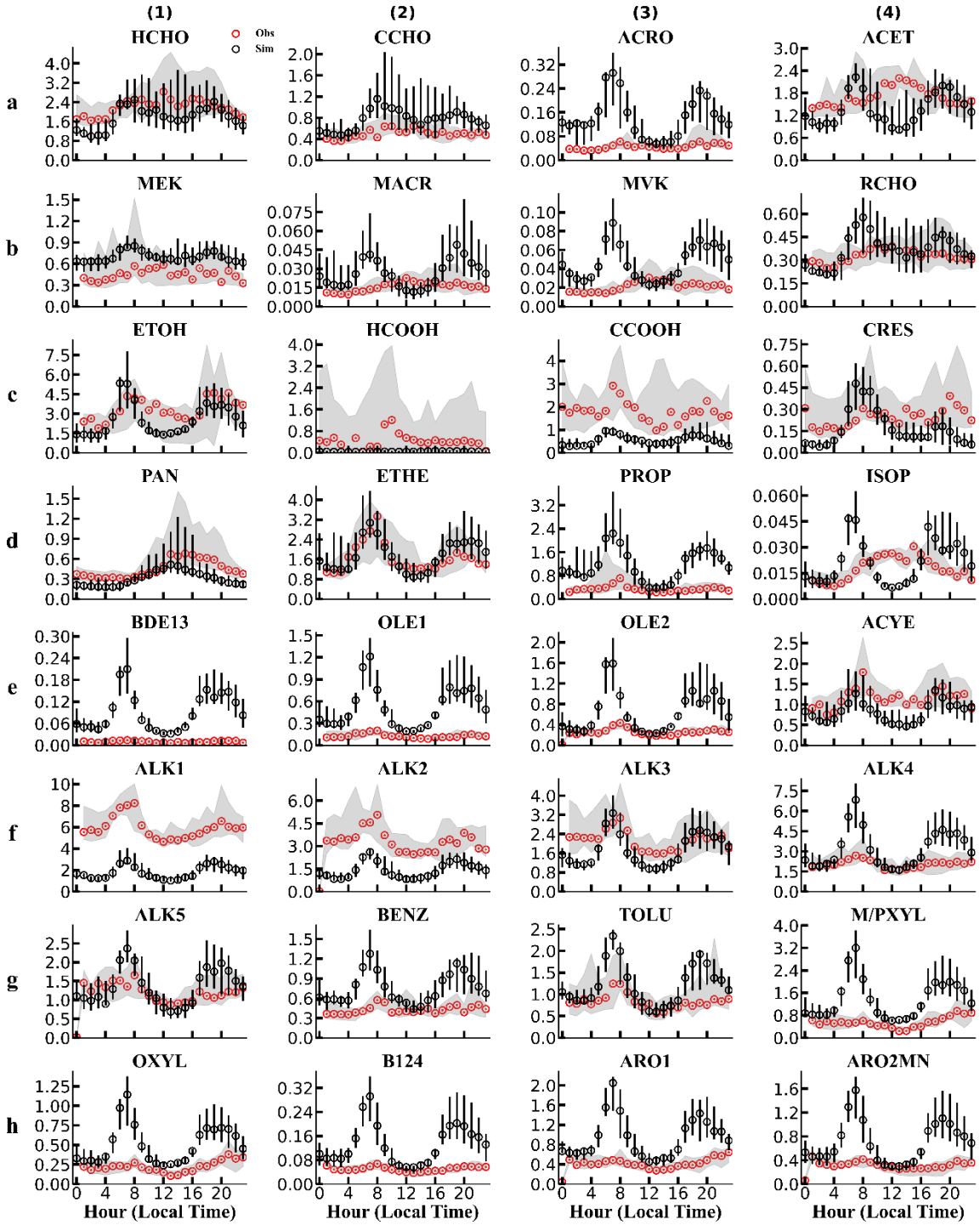

Figure S6. Diurnal variations of OVOCs and their precursors at SAES in EP2 (ppb). Red and black circles indicate the median observed and model-predicted values, respectively; shaded areas and black bars represent the 25th–75th percentile ranges for observations and model predictions, respectively.

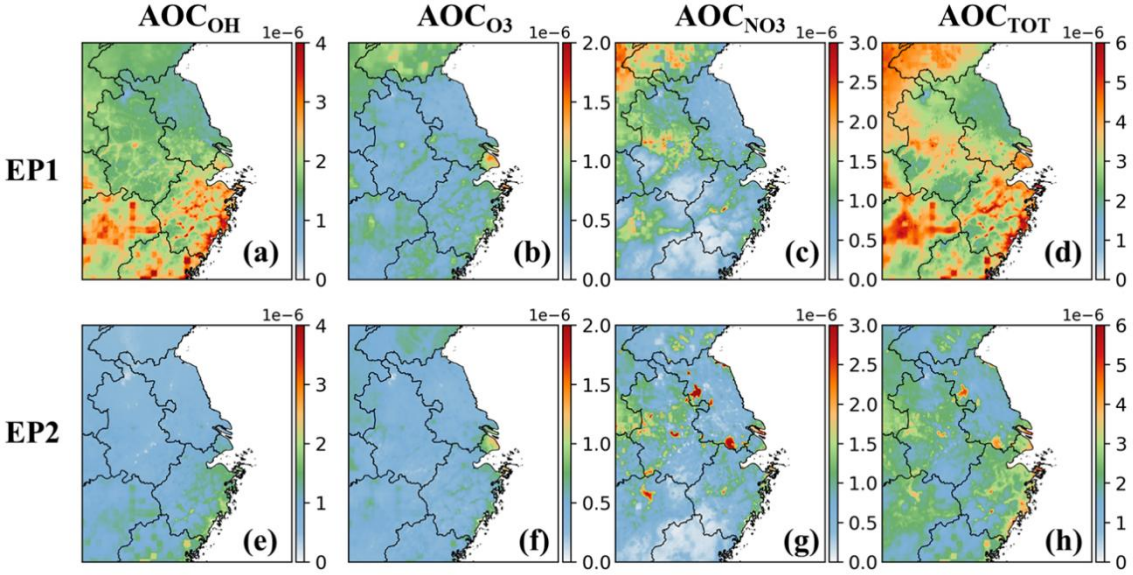

Figure S7. Atmospheric oxidation capacity (AOC) during the two episodes, contributed by OH radicals (AOC_{OH}; a, e), O_3 (AOC_{O3}; b, f), NO_3 radicals (AOC_{NO3}; c, g), and total AOC (AOC_{TOT}; d, h) (s^{-1}). AOC was calculated following Qin et al[1].

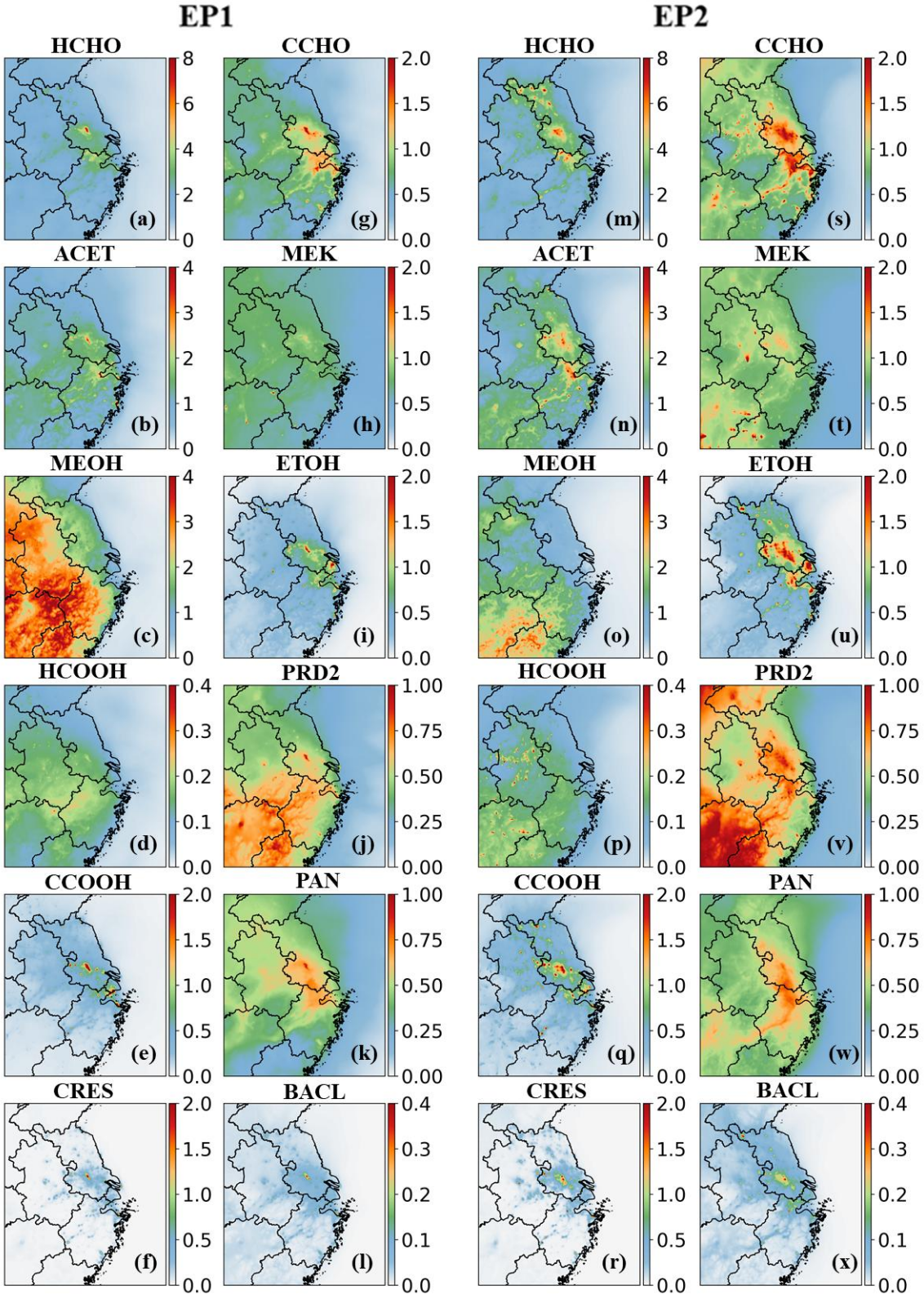

Figure S8. Spatial distributions of major OVOC species in EP1 (a−l) and EP2 (m−x) (ppb).

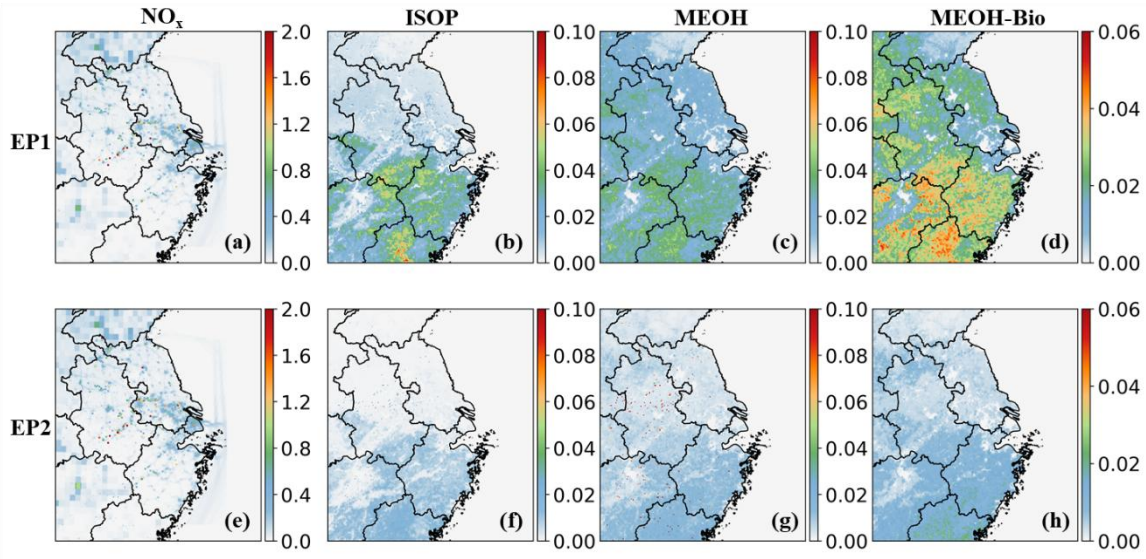

Figure S9. Average emission rates of NO_x, isoprene, MEOH, and biogenic MEOH during EP1 and EP2. Units are mole s^{-1}.

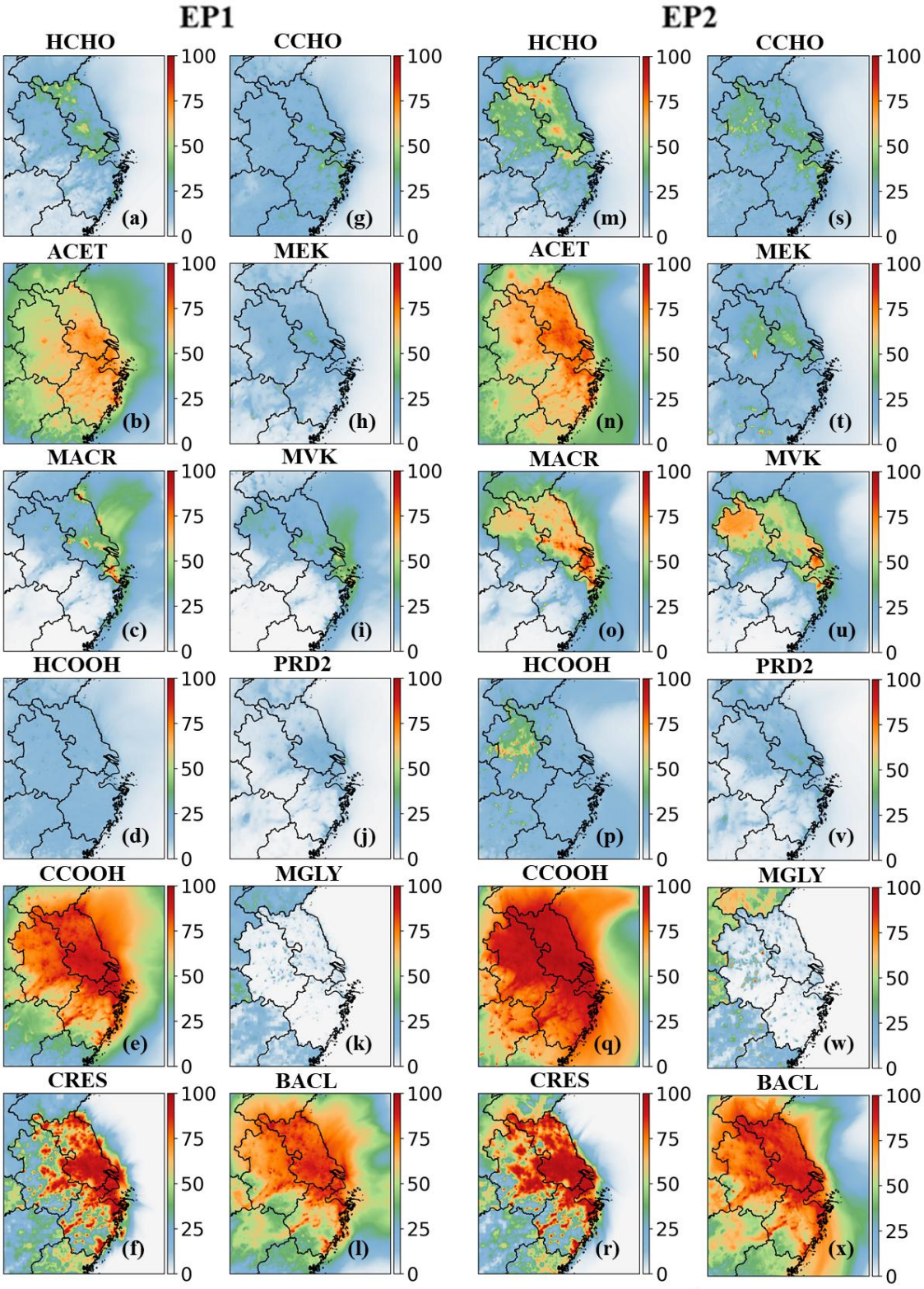

Figure S10. Emission contributions to individual OVOC species in EP1 (a−l) and EP2 (m−x).

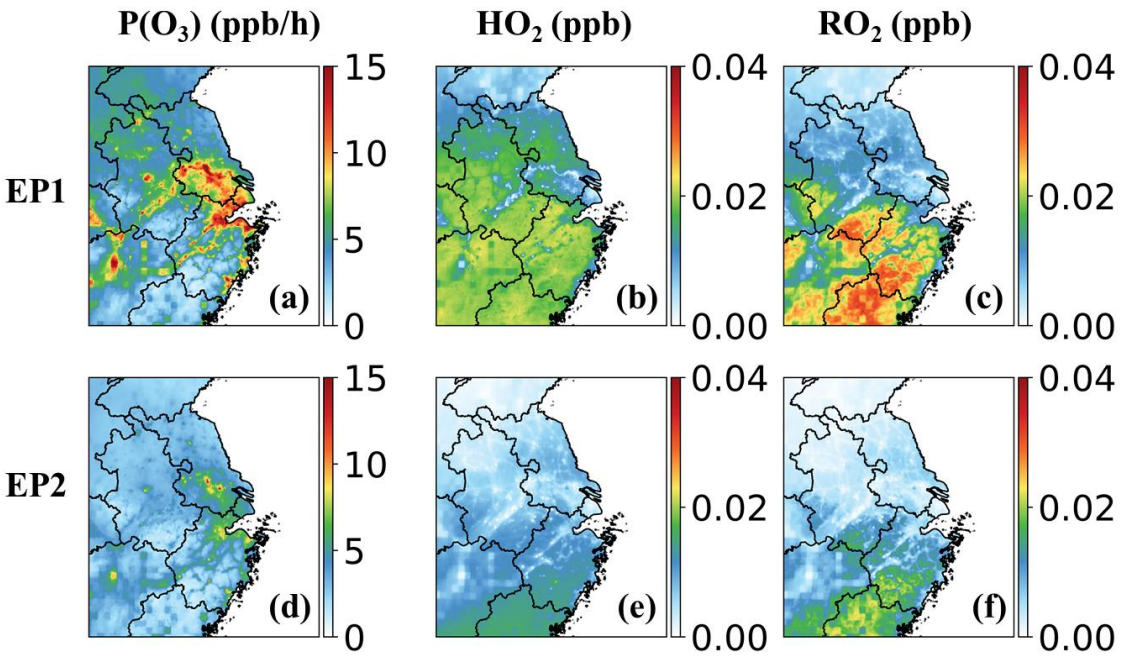

Figure S11. Average daytime ozone production rates ($P(O_3)$, a, d), HO_2 concentrations (b, e), and RO_2 concentrations (c, f) during EP1 and EP2.

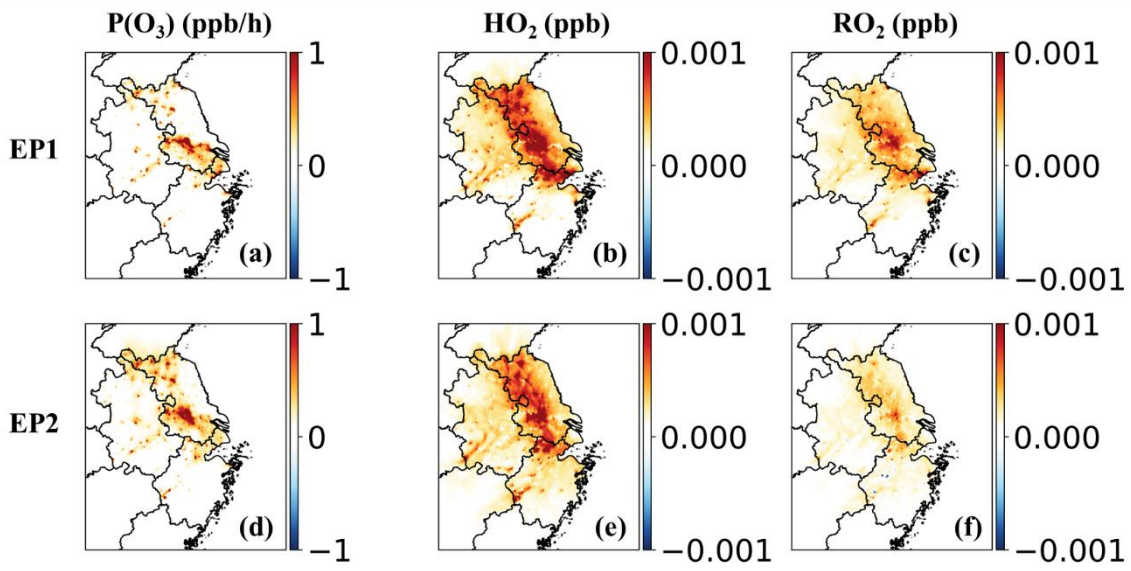

Figure S12. Contributions of OVOCs emitted from industrial processes to the daytime ozone production rate ($P(O_3)$, ppb h^{-1}) and HO_2 and RO_2 radical concentrations (ppb) during EP1 and EP2. The contributions are quantified as the differences between the base case and a sensitivity case in which OVOC emissions from the corresponding sources are set to zero.

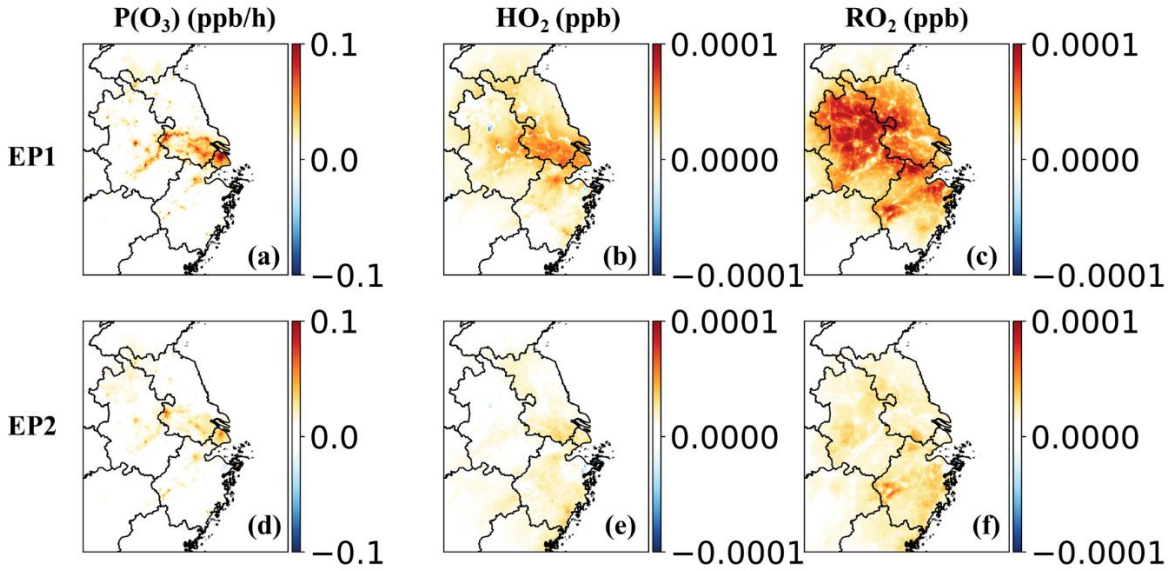

Figure S13. Same as Fig. S12 but for OVOCs emitted from residential sources.

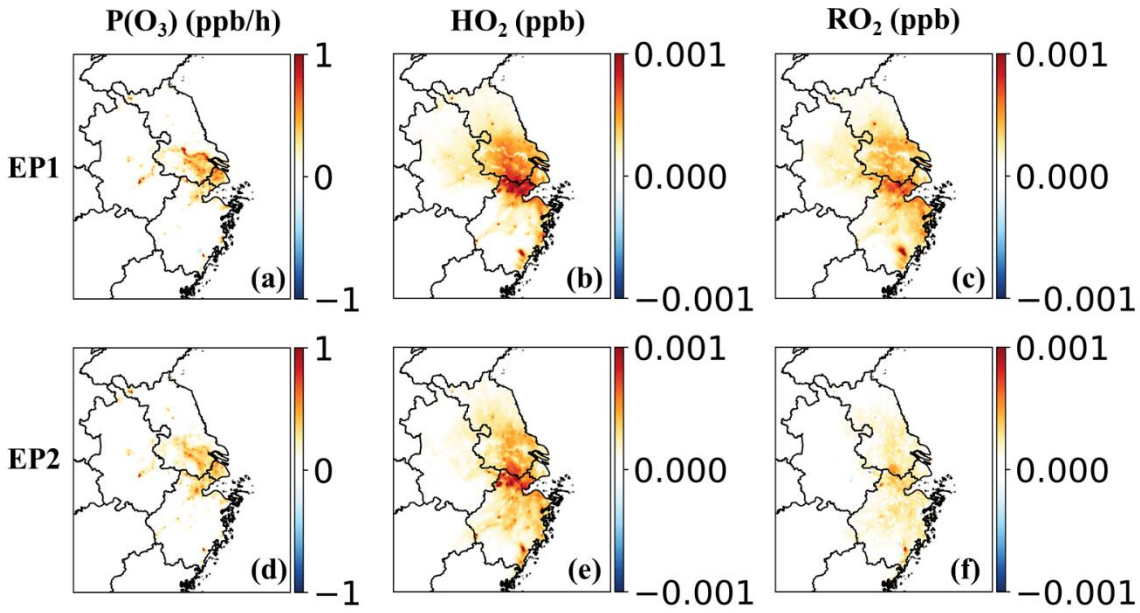

Figure S14. Same as Fig. S12 but for OVOCs emitted from solvent use sources.

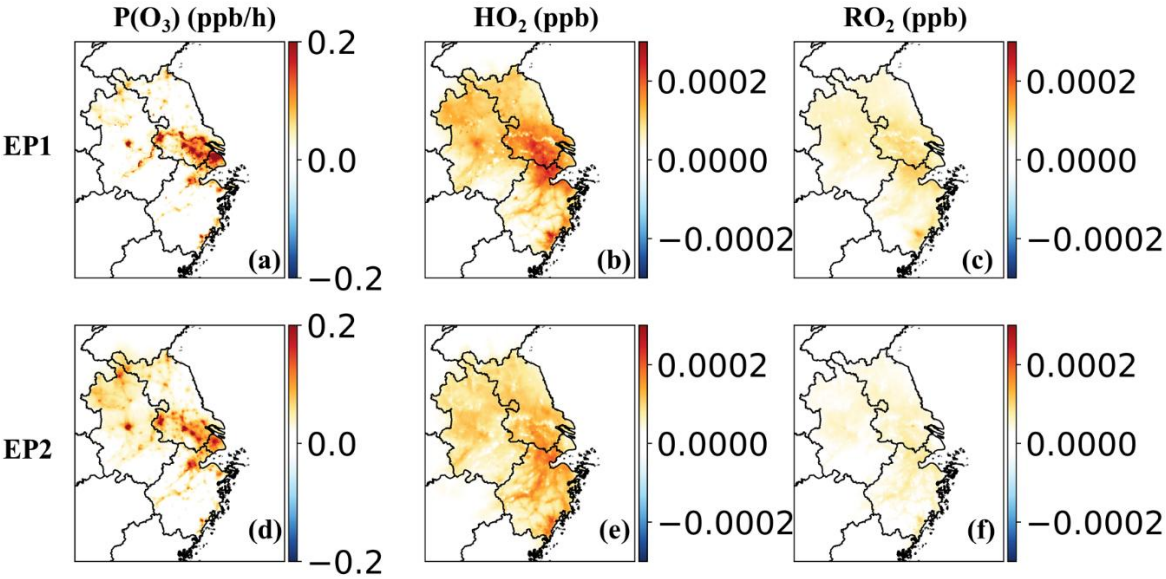

Figure S15. Same as Fig. S12 but for OVOCs emitted from transportation sources.

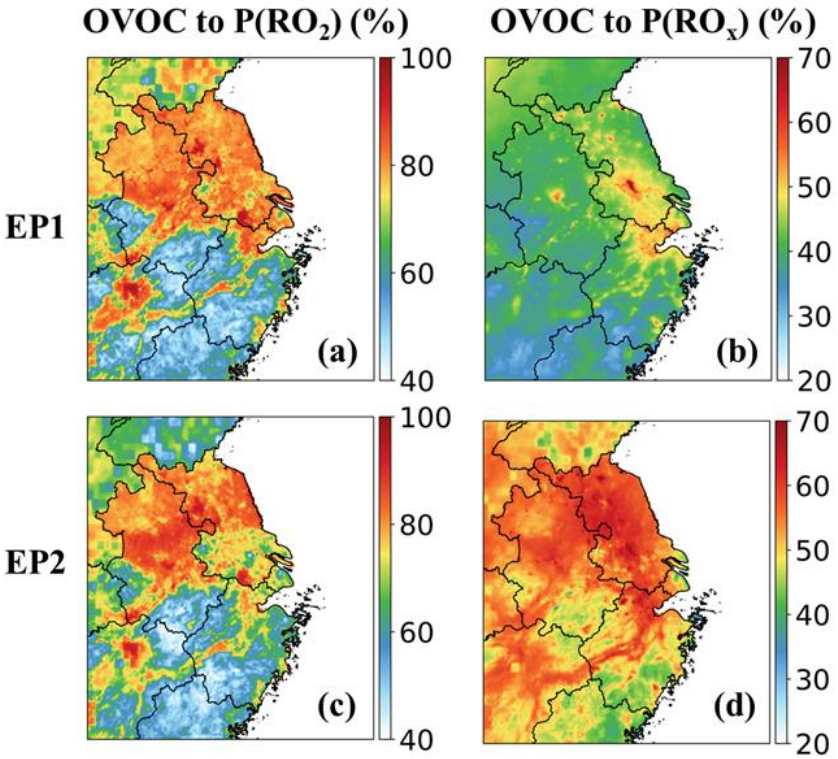

Figure S16. Contributions of OVOCs to the daytime primary RO_2 and RO_x production during EP1 and EP2.

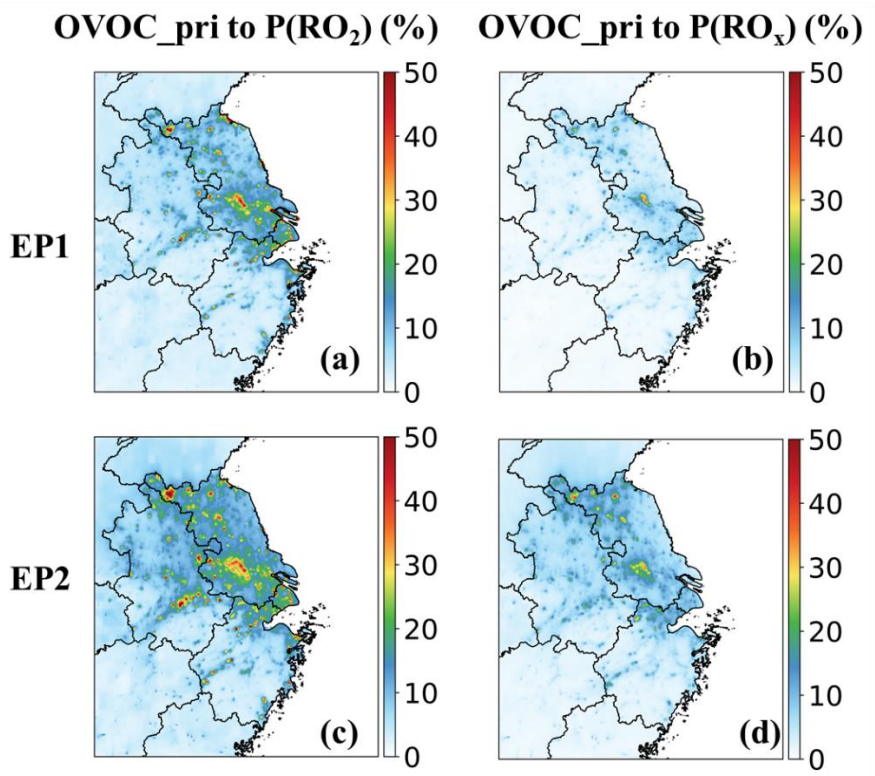

Figure S17. Contributions of primary OVOCs to total primary RO_2 (a, c) and RO_x (b, d) production during the daytime of EP1 and EP2.

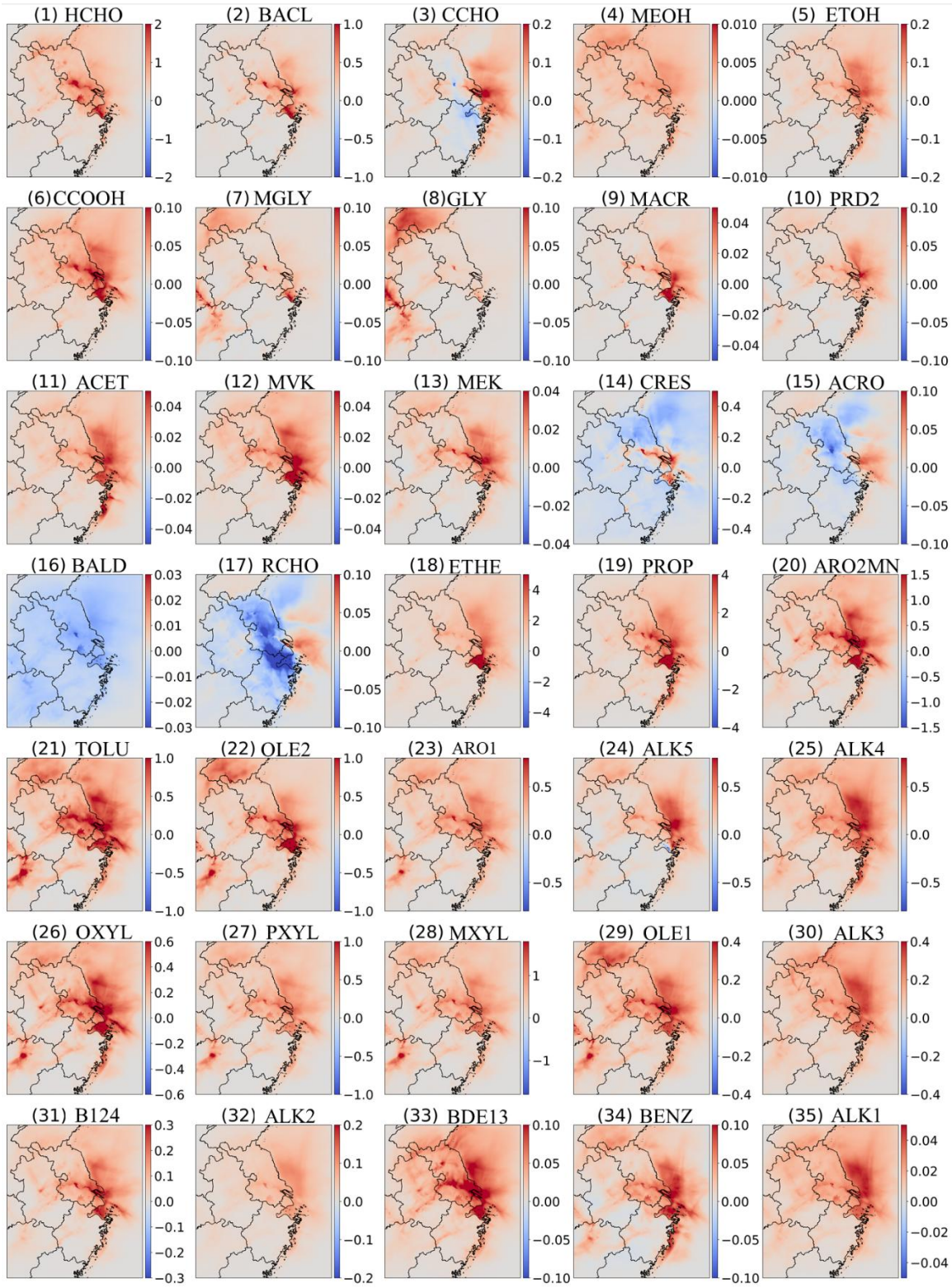

Figure S18. Daytime average ozone variations influenced by primary OVOCs and VOC precursors from April 1 to 7, 2019 (ppb).

Table S1. Definitions of OVOCs and other VOC species used in the model.

Species	Definition
HCHO	Formaldehyde
CCHO	Acetaldehyde
ACRO	Acrolein
ACET	Acetone
MACR	Methacrolein
MEK	Ketones and other non-aldehyde oxygenated products which react with OH radicals faster than 5×10^{-13} but slower than 5×10^{-12} cm^3 $molec^{-1}$ sec^{-1}. (Based on the mechanism for methyl ethyl ketone).
MVK	Methyl Vinyl Ketone
RCHO	Lumped C_3+ Aldehydes (mechanism based on propionaldehyde)
PRD2	Ketones and other non-aldehyde oxygenated products which react with OH radicals faster than 5×10^{-12} cm^3 $molec^{-1}$ sec^{-1}.
GLY	Glyoxal
MGLY	Methylglyoxal
HCOOH	Formic acid
CCOOH	Acetic acid
PAN	Peroxyacetyl Nitrate
RNO3	Lumped organic nitrates
AFG1	Lumped photoreactive monounsaturated dicarbonyl aromatic fragmentation products that photolyze to form radicals
AFG2	Lumped photoreactive monounsaturated dicarbonyl aromatic fragmentation products that photolyze to form non-radical products
AFG3	Lumped diunsaturated dicarbonyl aromatic fragmentation product
MEOH	Methanol
ETOH	Ethanol

CRES	Phenols and Cresols
BACL	Biacetyl
BALD	Aromatic aldehydes (e.g., benzaldehyde)
IPRD	Lumped isoprene product species
ETHE	Ethene
PROP	Propene
ISOP	Isoprene
BDE13	1,3-Butadiene
OLE1	Alkenes (other than ethene) with $k_{OH} < 7\times10^4$ ppm^{-1} min^{-1}.
OLE2	Alkenes with $k_{OH} > 7\times10^4$ ppm^{-1} min^{-1}.
ACYE	Acetylene
ALK1	Alkanes and other non-aromatic compounds that react only with OH, and have k_{OH} between 2×10^2 and 5×10^2 ppm^{-1} min^{-1}. (Primarily ethane)
ALK2	Alkanes and other non-aromatic compounds that react only with OH, and have k_{OH} between 5×10^2 and 2.5×10^3 ppm^{-1} min^{-1}. (Primarily propane and acetylene)
ALK3	Alkanes and other non-aromatic compounds that react only with OH, and have k_{OH} between 2.5×10^3 and 5×10^3 ppm^{-1} min^{-1}.
ALK4	Alkanes and other non-aromatic compounds that react only with OH, and have k_{OH} between 5×10^3 and 1×10^4 ppm^{-1} min^{-1}.
ALK5	Alkanes and other non-aromatic compounds that react only with OH, and have k_{OH} greater than 1×10^4 ppm^{-1} min^{-1}.
ARO1	Aromatics with $k_{OH} < 2\times10^4$ ppm^{-1} min^{-1}.
ARO2MN	Aromatics with $k_{OH} > 2\times10^4$ ppm^{-1} min^{-1}, excluding naphthalene
BENZ	Benzene
TOLU	Toluene
OXYL	o-Xylene
MXYL	m-Xylene
PXYL	p-Xylene
B124	1,2,4-Trimethyl benzene

Table S2. Comparison of source-specific contributions of different OVOC species to total VOCs between the 2017 and 2019 YRD emission inventories. ALD, KET, ALH, and EST denote aldehydes, ketones, alcohols, and esters, respectively.

Source[a]	Emission Inventory	ALD	KET	ALH	EST	Others	Total OVOCs
INB	2017	4.65%	0.78%	3.68%	1.14%	1.81%	12.1%
	2019	5.37%	1.27%	1.98%	0.78%	2.71%	12.1%
INP	2017	6.06%	4.65%	11.3%	4.58%	5.77%	32.3%
	2019	12.6%	5.58%	4.17%	2.74%	14.2%	39.2%
RES	2017	1.16%	5.16%	6.09%	0.51%	2.82%	15.7%
	2019	1.16%	5.16%	6.09%	0.51%	2.82%	15.7%
RBB	2017	24.1%	13.5%	0.54%	0.01%	0.08%	38.2%
	2019	25.9%	17.6%	0.00%	0.00%	1.12%	44.6%
COK	2017	12.7%	2.33%	0.00%	0.00%	0.08%	15.1%
	2019	12.7%	2.33%	0.00%	0.00%	0.08%	15.1%
NRD	2017	2.72%	2.72%	6.67%	2.07%	4.32%	18.5%
	2019	2.72%	2.72%	6.67%	2.07%	4.32%	18.5%
GVE	2017	0.82%	1.64%	6.47%	2.73%	4.09%	15.8%
	2019	7.63%	2.57%	1.42%	0.29%	3.12%	15.0%
DVE	2017	11.8%	6.40%	2.25%	8.13%	3.98%	32.5%
	2019	21.0%	2.13%	0.11%	2.46%	31.2%	56.9%
POW	2017	4.56%	2.06%	0.00%	0.00%	0.02%	6.64%
	2019	4.56%	2.06%	0.00%	0.00%	0.02%	6.64%
SHP	2017	2.92%	9.71%	2.65%	3.10%	0.52%	18.9%
	2019	2.92%	9.71%	2.65%	3.10%	0.52%	18.9%

[a]INP: industry process; INB: industrial boiler and kiln; RES: residential emissions excluding biomass burning; RBB: residential biomass burning; COK: cooking; GVE: gasoline vehicle; DVE: diesel vehicle; NRD: non-road machine; POW: power plant; SHP: ship emissions)

Table S3. Statistical metrics of meteorological parameters in Shanghai (SH), Nanjing (NJ), Hefei (HF), and Hangzhou (HZ)[a] in EP1 and EP2. Benchmark values are based on Emery et al[2].

Episode	Stations	Factor	MB	ME	RMSE	R	IOA
EP1	SH	T	-0.97	1.53	2	0.92	0.95
		RH	2.03	9.50	12.2	0.83	0.9
		WD	-5.63	92.1	139.7	0.30	0.62
		WS	1.34	1.54	1.79	0.58	0.63
	NJ	T	-0.43	2.21	1.81	0.95	0.97
		RH	-0.81	9.98	10.6	0.86	0.92
		WD	48.8	82.3	117.3	0.38	0.66
		WS	2.39	2.49	1.41	0.68	0.78
	HF	T	0.68	1.76	2.32	0.93	0.96
		RH	-10.7	14.1	18.7	0.76	0.81
		WD	9.82	89.9	133.0	0.27	0.61
		WS	0.08	1.09	1.41	0.70	0.8
	HZ	T	1.6	2.26	1.5	0.93	0.96
		RH	-7.35	11.0	11.5	0.78	0.88
		WD	9.01	86.9	147.4	0.28	0.62
		WS	1.05	1.65	1.32	0.60	0.77
EP2	SH	T	-0.65	1.44	3.04	0.82	0.9
		RH	-0.94	8.12	12.81	0.78	0.88
		WD	-35.2	66.4	116.8	0.26	0.55
		WS	0.6	1.16	2.88	0.51	0.49
	NJ	T	1.04	2.26	3.18	0.85	0.9
		RH	-2.08	11.3	14.3	0.76	0.86
		WD	25.2	74.3	114.6	0.29	0.61
		WS	1.47	1.98	2.51	0.36	0.56
	HF	T	-0.17	1.1	3.31	0.87	0.91
		RH	0.55	8.88	14.2	0.80	0.86
		WD	-26.0	97.8	125.2	0.24	0.58
		WS	-0.31	1.01	2.16	0.53	0.67
	HZ	T	0.18	2.73	3.62	0.80	0.89
		RH	-3.78	11.5	15.3	0.68	0.82
		WD	-11.3	97.4	132.9	0.14	0.52
		WS	1.51	1.92	2.53	0.33	0.49

[a] The locations of these stations are indicated in Figure S1. Benchmark values are MB≤±0.5 K, ME≤2 K for T; MB≤±10 deg, ME≤±30 deg for WD; MB≤±0.5 m/s, RMSE≤2 m/s for WS.

Table S4. Statistical metrics of MDA8 O_3 in selected cities in the YRD. Benchmark values are based on Emery et al[3].

Site	Episode	NMB	NME	RMSE	R	IOA
SH	EP1	0.031	0.33	22.3	0.37	0.65
	EP2	0.068	0.20	12.5	0.30	0.54
HF	EP1	0.23	0.32	21.7	0.44	0.59
	EP2	0.50	0.55	19.0	0.14	0.43
BB	EP1	0.18	0.29	20.2	0.37	0.55
	EP2	0.23	0.32	13.4	0.47	0.64
MAS	EP1	0.17	0.29	20.4	0.41	0.55
	EP2	0.29	0.36	14.3	0.46	0.56
NJ	EP1	0.22	0.35	24.2	0.34	0.53
	EP2	0.22	0.29	11.6	0.53	0.57
WX	EP1	0.19	0.33	23.5	0.38	0.57
	EP2	0.38	0.40	18.1	0.52	0.56
XZ	EP1	0.034	0.20	15.4	0.51	0.69
	EP2	0.28	0.29	11.2	0.70	0.68
YC	EP1	-0.11	0.19	15.1	0.67	0.76
	EP2	0.13	0.19	9.54	0.61	0.68
LYG	EP1	-0.14	0.22	16.1	0.64	0.71
	EP2	0.24	0.28	11.6	0.72	0.73
HZ	EP1	0.35	0.46	29.8	0.23	0.52
	EP2	0.55	0.60	24.9	0.34	0.50
NB	EP1	0.039	0.31	22.2	0.20	0.51
	EP2	0.19	0.23	12.6	0.60	0.68
JX	EP1	0.23	0.36	26.5	0.20	0.51
	EP2	0.35	0.40	18.8	0.50	0.57
JH	EP1	0.11	0.28	17.7	0.24	0.50
	EP2	0.26	0.34	17.1	0.60	0.62
LS	EP1	0.14	0.22	14.1	0.32	0.57
	EP2	0.032	0.19	11.8	0.56	0.69
Benchmark		$\leq\pm0.15$	<0.25		>0.5	

Table S5. Statistical metrics of OVOCs and VOC precursors in Shanghai in EP1 and EP2.

Species	Episode	Obs (ppb)	Pred (ppb)	NMB	NME	RMSE	R	IOA
HCHO	EP1	2.52	1.85	-0.26	0.39	1.38	0.55	0.70
	EP2	2.58	2.05	-0.21	0.32	1.10	0.72	0.79
CCHO	EP1	1.25	0.85	-0.32	0.49	0.78	0.46	0.63
	EP2	0.56	0.93	0.64	0.74	0.60	0.60	0.56
ACRO	EP1	0.15	0.090	-0.40	0.55	0.11	0.16	0.47
	EP2	0.053	0.15	1.75	1.81	0.13	0.46	0.33
ACET	EP1	5.75	1.40	-0.76	0.76	5.44	0.25	0.44
	EP2	1.89	1.54	-0.19	0.43	1.11	0.39	0.61
MACR	EP1	0.030	0.037	0.24	0.91	0.045	0.052	0.21
	EP2	0.018	0.032	0.79	1.06	0.027	0.36	0.43
MEK	EP1	1.07	0.70	-0.35	0.45	0.84	0.27	0.46
	EP2	0.64	0.75	0.17	0.59	0.49	0.51	0.58
MVK	EP1	0.050	0.052	0.042	0.73	0.062	0.071	0.28
	EP2	0.026	0.053	1.03	1.17	0.043	0.48	0.49
RCHO	EP1	0.76	0.35	-0.53	0.56	0.49	0.36	0.46
	EP2	0.36	0.40	0.11	0.35	0.17	0.61	0.73
ETOH	EP1	9.56	1.82	-0.81	0.81	8.98	0.28	0.41
	EP2	3.24	2.97	-0.084	0.80	3.58	0.039	0.37
HCOOH	EP1	0.15	0.093	-0.37	0.64	0.12	0.19	0.39
	EP2	1.95	0.072	-0.96	0.99	3.93	0.37	0.36
CCOOH	EP1	1.88	0.48	-0.75	0.75	1.87	0.31	0.44
	EP2	2.59	0.66	-0.75	0.76	3.15	0.32	0.44
CRES	EP1	0.070	0.14	1.05	1.43	0.16	0.23	0.19

	EP2	0.41	0.20	-0.51	0.72	0.53	0.18	0.39
PAN	EP1	0.99	0.47	-0.53	0.69	0.88	0.40	0.56
	EP2	0.61	0.39	-0.35	0.40	0.38	0.76	0.79
ETHE	EP1	1.52	1.73	0.14	0.69	1.43	0.26	0.53
	EP2	1.96	2.28	0.16	0.55	2.11	0.34	0.51
PROP	EP1	0.38	0.95	1.47	1.61	0.88	0.44	0.44
	EP2	0.58	1.39	1.39	1.57	1.26	0.51	0.57
ISOP	EP1	0.038	0.017	-0.55	0.66	0.047	0.067	0.37
	EP2	0.019	0.024	0.23	0.79	0.022	0.22	0.44
OLE1	EP1	0.15	0.35	1.33	1.43	0.29	0.25	0.31
	EP2	0.14	0.60	3.31	3.31	0.65	0.35	0.16
OLE2	EP1	0.28	0.40	0.44	0.77	0.35	0.28	0.48
	EP2	0.28	0.75	1.71	1.77	0.84	0.37	0.21
BDE13	EP1	0.022	0.061	1.74	2.02	0.063	0.12	0.26
	EP2	0.011	0.11	8.80	8.80	0.14	0.30	0.078
ACYE	EP1	1.36	0.83	-0.39	0.51	1.04	0.24	0.50
	EP2	1.35	1.01	-0.25	0.54	1.02	0.34	0.54
ALK1	EP1	8.30	1.58	-0.81	0.81	8.03	0.20	0.41
	EP2	6.83	2.03	-0.70	0.70	5.64	0.45	0.44
ALK2	EP1	4.29	1.17	-0.73	0.73	4.40	0.26	0.45
	EP2	4.22	1.55	-0.63	0.65	3.82	0.43	0.47
ALK3	EP1	2.60	1.29	-0.51	0.56	2.27	0.24	0.45
	EP2	2.62	1.91	-0.27	0.47	1.80	0.36	0.56
ALK4	EP1	3.22	2.18	-0.32	0.53	2.83	0.17	0.43
	EP2	2.42	3.58	0.48	0.69	2.69	0.33	0.45
ALK5	EP1	3.21	1.20	-0.63	0.66	2.54	0.19	0.44

	EP2	1.34	1.68	0.26	0.62	1.86	0.28	0.33
ARO1	EP1	0.61	0.65	0.062	0.59	0.50	0.16	0.47
	EP2	0.45	1.03	1.30	1.40	0.90	0.18	0.30
ARO2MN	EP1	0.24	0.48	0.97	1.14	0.39	0.20	0.29
	EP2	0.32	0.78	1.45	1.54	0.75	0.22	0.25
BENZ	EP1	0.49	0.56	0.15	0.55	0.38	0.29	0.54
	EP2	0.47	0.81	0.73	0.80	0.56	0.41	0.43
TOLU	EP1	1.19	0.81	-0.32	0.54	1.18	0.27	0.46
	EP2	1.11	1.28	0.16	0.55	0.93	0.43	0.64
M/PXYL	EP1	0.56	0.92	0.64	0.99	0.79	0.22	0.44
	EP2	0.63	1.56	1.48	1.58	1.52	0.21	0.27
OXYL	EP1	0.24	0.34	0.45	0.84	0.29	0.21	0.45
	EP2	0.25	0.57	1.29	1.41	0.55	0.25	0.29
B124	EP1	0.045	0.091	1.03	1.17	0.073	0.28	0.32
	EP2	0.053	0.15	1.77	1.80	0.15	0.27	0.17

Table S6. Proportions of different OVOC species in total primary OVOCs from the anthropogenic sources across the YRD during the two episodes.

Species	EP1(%)	EP2(%)
CRES	21.6	21.9
HCHO	15.9	15.9
ACET	14.4	14.3
CCOOH	12.5	12.5
ETOH	9.52	9.41
RCHO	5.78	5.75
CCHO	5.55	5.55
PRD2	3.54	3.58
MEK	3.54	3.53
ACRO	2.76	2.75
BACL	2.32	2.35
MEOH	0.71	0.71
MVK	0.58	0.56
MACR	0.53	0.52
BALD	0.45	0.44
HCOOH	0.16	0.16
MGLY	0.11	0.11
GLY	0.05	0.05

Table S7. Molar yields of NO_2 from RO_2 and NO reactions that form alkyl nitrate coproducts in SAPRC07tic.

Reactants	Molar yield of NO_2	Description
TERPNRO2 + NO	0.827	Monoterpene + NO_3 peroxy radical (TERPNRO2) reaction with NO
ISOPO2 + NO	0.883	Isoprene + OH peroxy radical (ISOPO2) reaction with NO
NISOPO2 + NO	1.0	Isoprene + NO_3 peroxy radical (NISOPO2) reaction with NO
ISOPNOOB + NO	1.0	β-hydroxy isoprene nitrates + OH peroxy radical (ISOPNOOB) reaction with NO
ISOPNOOD + NO	1.0	δ-hydroxy isoprene nitrates + OH peroxy radical (ISOPNOOD) reaction with NO
MVKOO + NO	0.89	MVK + OH peroxy radical (MVKOO) reaction with NO
MACROO + NO	0.85	MACR + OH peroxy radical (MACROO) reaction with NO
NIT1NO3OOA + NO	1.0	C_5 carbonyl nitrates + NO_3 acyl peroxy radical via abstraction of aldehydic H (NIT1NO3OOA) reaction with NO
NIT1NO3OOB + NO	0.94	C_5 carbonyl nitrates + NO_3 peroxy radical via addition to double bond (NIT1NO3OOB) reaction with NO
NIT1OHOO + NO	0.934	C_5 carbonyl nitrates + OH peroxy radical (NIT1OHOO) reaction with NO

References

1. Qin, M.; Hu, A.; Mao, J.; Li, X.; Sheng, L.; Sun, J.; Li, J.; Wang, X.; Zhang, Y.; Hu, J., PM2.5 and O3 relationships affected by the atmospheric oxidizing capacity in the Yangtze River Delta, China. *Science of the Total Environment* **2022,** *810*, 152268.

2. Emery, C.; Edward, T.; and Yarwood, G. Enhanced Meteorological Modeling and Performance Evaluation for Two Texas Ozone Episodes. Report to the Texas Natural Resources Conservation Commission, ENVIRON International Corporation, Novato, CA, 2001.

3. Emery, C.; Liu, Z.; Russell, A. G.; Odman, M. T.; Yarwood, G.; Kumar, N. Recommendations on statistics and benchmarks to assess photochemical model performance. *Journal of the Air & Waste Management Association* 2017, 67 (5), 582-598. DOI: 10.1080/10962247.2016.1265027.